On the Structure and Oscillations of the First Stars

Thiago Ferreira[1], Earl P. Bellinger[1], Ebraheem Farag[1], and Christopher J. Lindsay[1]

[1]Yale University | **Contact**: **thiago.dossantos@yale.edu**

Low-mass Population III (Pop III) stars are expected to survive in the Milky Way halo and/or its dwarf satellites, however, their identification remains elusive [1-4]. Surface abundances from internal mixing (e.g., element diffusion and dredge-up) can mimic second-generation chemical signatures, obscuring their primordial origin. As these stars differ fundamentally in opacity, convective structure, and evolutionary pathways due to their metal-free composition, asteroseismology may offer a promising, independent probe of their interiors. **In this study, we assess whether their oscillation spectra reveal unique seismic signatures that could distinguish Pop III survivors from metal-rich stars of similar mass and evolutionary stage.**

EVOLUTIONARY TRACKS. Pop III stellar models are hotter, more compact, and luminous than metal-rich counterparts. Models with $M \lesssim 0.75\ M_\odot$ remain on the MS today, while more massive ones evolve to WDs. For $M \gtrsim 0.85\ M_\odot$, deep dredge-up and shell mergers during the asymptotic giant branch bring to the surface CNO elements, producing C/N-enhanced ultra metal-poor stars by 10 Gyr. Extreme horizontal branch-like phases emerge from off-centre He ignition under degenerate conditions, enabled by mass loss (up to $10^{-7}\ M_\odot\ \mathrm{yr}^{-1}$). These helium-burning phases are UV-bright and short-lived ($\sim 20-60$ Myr) and may leave fossil signatures in old white dwarf populations.

OSCILLATION SPECTRA were computed using GYRE [7] focusing on a 0.85 $M_\odot$ case study star at the sub-giant (SG) and red giant branches (RGB). Oscillation modes reveal distinct seismic fingerprints driven by Pop III stars zero-metallicity interiors:

(a) The absence of metals drastically reduces opacity, steepening internal temperature gradients and producing more compact, denser cores, with higher sound speeds; **(b)** Pop III stars show larger $\Delta\nu$ than metal-poor stars at a fixed model mass, reflecting compact structure and higher mean densities; **(c)** Elevated ratios $r_{02} = \delta\nu_{02}/\Delta\nu$ indicate sharper sound-speed contrasts between core and envelope, a hallmark of primordial composition and efficient radiative energy transport; **(d)** Gravity modes in Pop III stars exhibit higher normalized inertias, indicating strong trapping in the compact, stratified core and lower surface amplitudes. This contrasts with metal-poor stars where metals smooth gradients and weaken mode trapping; **(e)** Buoyancy frequency profiles reveal pronounced peaks in Pop III stars, evidencing strong stratification and efficient gravity-mode cavities, in contrast to the smoother profiles in metal-poor models; **(f) Pop III stars have higher $\psi \equiv \Delta\nu/\Delta\Pi_1$ at fixed $\Delta\Pi_1$ during the RGB due to slower core evolution and more modest chemical gradients, distinguishing them from metal-poor counterparts (e.g., [9, 10]).**

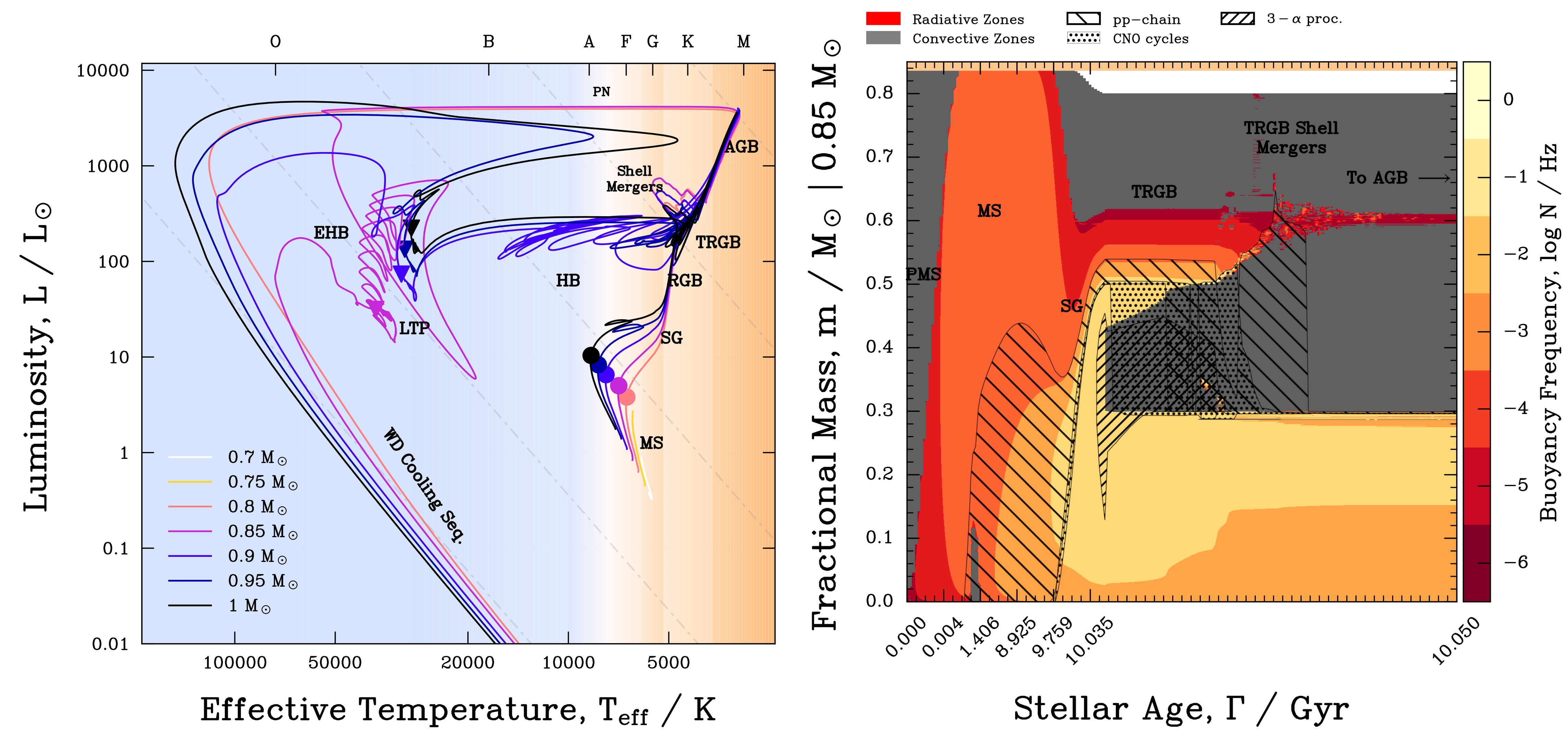

Figure 1. HR diagram for low-mass Pop III stars with stellar radii (dashed), spectral type regions (background shading), and evolutionary phases (right). Kippenhahn diagram for a $0.85\ M_\odot$ model, showing convective boundaries, core helium burning, and structural transitions (left).

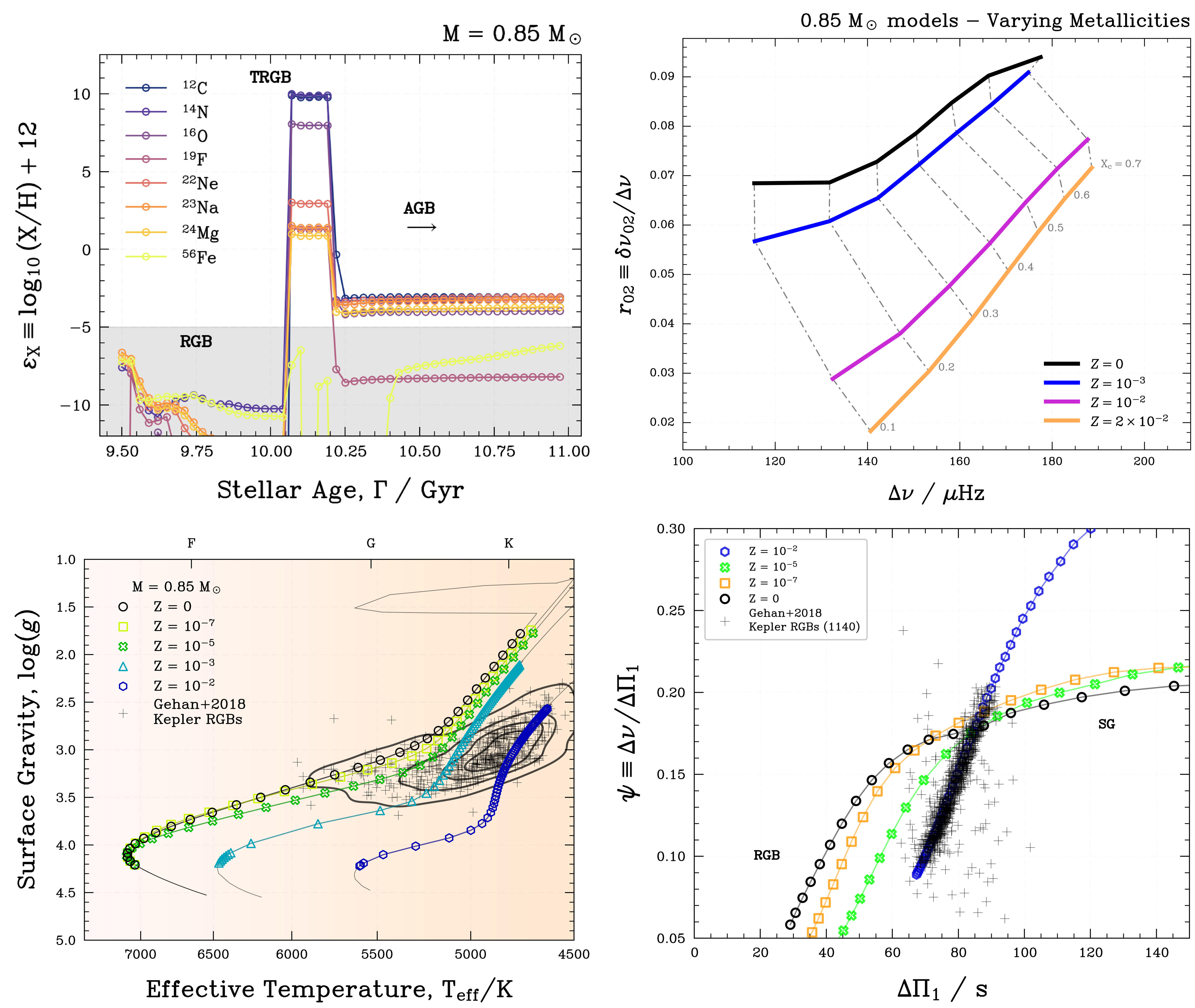

Figure 2. **Top left**: Evolution of surface chemical abundances ($\varepsilon_X = \log_{10}(X/H) + 12$) for several elements in a 0.85 $M_\odot$ star as a function of stellar age, with shell merger phases highlighted. The shaded grey region represents the approximate lower limit of surface abundances observed in extremely metal-poor stars (e.g., SMSS J031300.36-670839.3 with [Fe/H] ≈ -7.3 [11]). **Top right**: Evolution of the small frequency separation ratio $r_{02} \equiv \delta\nu_{02}/\Delta\nu$ vs. $\Delta\nu$ for 0.85 $M_\odot$ models at varying metallicities. **Bottom left**: Kiel diagram for 0.85 $M_\odot$ models at different metallicities. Crosses represent 1140 observed Kepler RGB stars from [10]. **Bottom right**: Seismic spacing ratio $\psi \equiv \Delta\nu/\Delta\Pi_1$ vs. $\Delta\Pi_1$ for varying metallicities. Lower-metallicity models show decreased ψ during late subgiant phases. Pop III stars, in particular, consistently exhibit higher ψ values throughout the RGB, reflecting weaker coupling between p- and g-mode cavities.

References: [1] Abel et al. (2000; ApJ 540, 39), [2] Komiya et al. (2016; ApJ 820, 59), [3] Hirano & Bromm (2017; MNRAS 470, 898), [4] Chandra & Schlaufman (2021; AJ 161, 197), [5] Paxton et al. (2011-2019; ApJS, 192, 220, 223, 234, 243), [6] Jermyn et al. (2023; ApJ 913, 72), [7] Townsend & Teitler (2013; MNRAS 435, 3406), [8] Mosser et al. (2012; A&A 540A, 143), [9] Buysschaert et al. (2016; A&A 588A, 82), [10] Gehan et al. (2018; A&A 616A, 24), [11] Keller et al. (2014; Nature 506, 463).